Iron- and erythropoietin-resistant anemia in a spontaneous breast cancer mouse model

Nuria Fabregas Bregolat,[1,2] Maja Ruetten,[3] Milene Costa da Silva,[4] Mostafa A. Aboouf,[1,2,5] Hyrije Ademi,[1,2] Nadine von Büren,[1,2] Julia Armbruster,[1,2] Martina Stirn,[6] Sandro Altamura,[4,7] Oriana Marques,[4,7] Josep M. Monné Rodriguez,[8] Victor J. Samillan,[9] Rashim Pal Singh,[10] Ben Wielockx,[10] Martina U. Muckenthaler,[4,7,11,12] Max Gassmann[1,13] and Markus Thiersch[1,2,13]

[1]Institute of Veterinary Physiology, Vetsuisse Faculty, University of Zurich, Zurich, Switzerland; [2]Center for Clinical Studies, Vetsuisse Faculty, University of Zurich, Zurich, Switzerland; [3]PathoVet AG, Pathology Diagnostic Laboratory, Tagelswangen ZH, Switzerland [4]Department of Pediatric Oncology, Hematology and Immunology, University of Heidelberg, Heidelberg, Germany; [5]Department of Biochemistry, Faculty of Pharmacy, Ain Shams University, Cairo, Egypt; [6]Clinical Laboratory, Department of Clinical Diagnostics and Services, Vetsuisse Faculty, University of Zurich, Zurich, Switzerland; [7]Molecular Medicine Partnership Unit, Heidelberg, Germany; [8]Laboratory for Animal Model Pathology, Institute of Veterinary Pathology, Vetsuisse Faculty, University of Zurich, Zurich, Switzerland [9]Universidad Le Cordon Bleu, School of Human Nutrition, Lima, Peru; [10]Institute of Clinical Chemistry and Laboratory Medicine, Carl Gustav Carus, TU Dresden, Germany; [11]Translational Lung Research Center Heidelberg (TLRC), German Center for Lung Research (DZL), University of Heidelberg, Heidelberg, Germany; [12]German Center for Cardiovascular Research, Partner Site, Heidelberg, Germany and [13]Zurich Center for Integrative Human Physiology (ZIHP), University of Zurich, Zurich, Switzerland

Correspondence:
Markus Thiersch
markus.thiersch@uzh.ch

Received: January 24, 2022.
Accepted: March 31, 2022.
Prepublished: April 7, 2022.

https://doi.org/10.3324/haematol.2022.280732

Supplemental Information

Iron- and erythropoietin-resistant anemia in a spontaneous breast cancer mouse model

Fabregas Bregolat et al.

Running Title: **Iron- and erythropoietin-resistant mice with AoC**

Methods

Animals

Trp53floxWapCre mice [1] were housed at 22±5 °C in a 12 h light/dark cycle and received water and food (standard rodent chow containing 250 mg/kg iron from Kliba Nafag, #3436, Switzerland) *ad libitum*. Tumor development in female Trp53^{flox}WapCre mice was monitored visually and by palpation when mice reached 18 weeks of age. Tumor length (L) and width (W) were measured using a caliper and tumor volume was calculated [$V=(LxW^2)/2$] [2]. In addition to the standard rodent chow (containing 250 mg/kg iron) (Kliba Nafag, #3436, Switzerland), some mice were kept on an iron sufficient diet (containing 50 mg/kg iron) (Kliba Nafag, #2222 modified, Switzerland), which did not exceed the daily iron demand. Mice were placed on this low iron diet either directly after weaning or after 15 weeks of age. Prior tissue isolation, blood was obtained from the right ventricle and mice were transcardially perfused with PBS. Isolated tissue was either immediately processed, snap frozen in liquid nitrogen or incubated for 48 h in 4% paraformaldehyde (PFA) for paraffin embedding. For histological analyses a hematoxylin-eosin staining was performed.

Hemoglobin, hematocrit, and hematology

Hemoglobin was measured from fresh whole blood by ABL800 (Radiometer RSCH GmbH, Switzerland) and hematocrit was manually measured in blood-filled heparin capillaries by determining the ratio of the volume occupied by red blood cells to the volume of whole blood after 5 min at 120 rpm in the microcentrifuge (HETTICH, Switzerland). Hematology, including erythrocytes was analyzed from whole blood by the Sysmex XT-2000iV (Sysmex Swiss AG, Switzerland).

Plasma metabolites

Fresh whole blood containing heparin was centrifuged at 2‘000 rpm for 10 minutes to isolate plasma that was processed immediately or snap frozen and stored at -80°C until analysis. Bilirubin, glucose, urea, creatinine, total protein, cholesterol, triglycerides, alkaline phosphatase, aspartate transaminase and alanine transaminase were analyzed by using the Roche Cobas Integra 800 device (Roche, Switzerland).

Erythropoietin treatment

Mice were subcutaneously (s.c.) injected with either 100 µl saline or with 1‘000 U/kg erythropoietin (Epoetin-beta; Recormon®, Roche) diluted in 100 µl saline directly after tumor detection trice a week until mice reached maximal tumor size.

Iron treatment

Mice were intravenously (i.v.) injected with either 100 µl saline or 13.8 as well as 20 mg/kg ferric carboxymaltose (Ferinject®, Vifor Pharma, Switzerland) diluted in 100 µl saline directly after tumor detection. The dosage was calculated by the Ganzoni formula [3] based on body weight (BW) and hemoglobin (Hb) levels as follows:

[Total iron deficit [mg] = BW [kg] x (target Hb - actual Hb) [g/dl] x 2.4) + storage iron [mg] with BW at the moment of tumor onset, target Hb referring to the upper 75% percentile of Hb values in tumor free mice and actual Hb referring to the lower 25% percentile of Hb values in terminal stage tumor mice.

Plasma and tissue iron

Plasma iron concentration was measured using a colorimetric bathophenanthroline assay (SFBC, Biolabo, France) and the unsaturated iron binding capacity was measured by UIBC assay (Biolabo, France). Total iron binding capacity (TIBC) was calculated TIBC (µg/dl) = SFBC (µg/dl) + UIBC (µg/dl) and transferrin saturation was calculated by Tsat(%) = SFBC / TIBC x 100. Non-heme iron content in tissues was measured by the bathophenanthroline method and normalized to weight of dry tissue [4].

Perls'-DAB enhanced staining and immunohistochemistry

Tissues were paraffin embedded after fixation with 4% paraformaldehyde for 24 hours and 5 µm sections were cut. After deparaffinization slides were stained with a potassium ferrocyanide/HCL solution (Sigma-Aldrich, Switzerland) followed by washing in demineralized water. After blocking with H_2O_2 (Sigma-Aldrich, Switzerland), slides were stained with 3,3-diaminobenzidinetetrahydrochloride (DAB) (Sigma-Aldrich, Switzerland) and counterstained with hematoxylin (Sigma-Aldrich, Switzerland). For Ki67 immunohistochemistry, tissue slides were incubated in 3% H_2O_2 (Sigma-Aldrich, Switzerland) and stained in the automated staining system Discovery (Ventana Medical Systems, Inc., USA) using a rabbit-anti-Ki67 antibody (# 790-4286, Roche, Switzerland) and the Discovery DAB Map detection kit (#760-124, Roche, Switzerland). For morphometric quantification of Ki67 cells in the liver, slides were scanned (NanoZoomer 2.0-HT; Hamamatsu, Hamamatsu City, Japan) and evaluated with an image analysis software (Visiopharm 2020.08.1.8403; Visiopharm, Hoersholm, Denmark). First the whole liver tissue was detected by Decision Forest classification method and outlined as region of interest (ROI). Subsequently, the Cell classification method was used to detected negative cells (blue) and positive cells (brown) within the ROI. The results were expressed as percentage of positive cells. For ferroportin

immunohistochemistry, tissue slides were stained using a rabbit-anti-metal transport protein MTP1 (Ferroportin) (# MTP11-A, Alpha Diagnostic, USA) and the Vectastain ABC kit (Vector Labs, USA) as well as the Vector AEC substrate (Vector Labs, USA). Prior incubation with the primary antibody, slides were incubated in 3% H_2O_2 (Sigma Aldrich, Switzerland) to block endogenous peroxidases followed by an antigen retrieval with Citra Plus solution (BioGenex, USA). Slides were counterstained with hematoxylin.

Bone marrow smears

Bone marrow smears were obtained from the medullar cavity of femurs using the paint brush technique [5]. Slides were air-dried and stained with a Giemsa staining. The cells were morphologically evaluated, and a differential count of the hematologic precursors was performed by light microscopy at 100x.

mRNA expression analysis by real time PCR and digital droplet PCR

RNA was extracted from snap frozen tissue by using the ReliaPrep® RNA Tissue Miniprep System (Promega) and RNA was either immediately processed or stored at -80°C. For cDNA synthesis we used the RevertAid Reverse Transcriptase (Thermo Fisher Scientific, Switzerland) as well as RiboLock RNase inhibitor (Thermo Fisher Scientific, Switzerland). Primers were designed with Primer3 [6] and all primer sequences are indicated in **Supplementary Table 1**. Real time PCR was performed in Thermocycler ABI7500 Fast (Applied Biosystems) using LightCycler 480 SYBR Green (Roche Applied Science, Switzerland) and relative gene expression was determined by the ΔΔCT method [7] with β-actin (*Actb*) as a reference gene. In addition, we quantified hepcidin (*Hamp1*) expression by a digital droplet PCR (QX100, ddPCR™, Biorad) with mouse specific TaqMan probes (ThermoFisher Scientific, Switzerland) against *Hamp1* (Mm04231240_s1) and *Actb* (Mm00607939_s1).

Plasma cytokines, ferritin and hepcidin

Fresh whole blood containing heparin was centrifuged at 2000 rpm for 10 minutes to isolate plasma that was processed immediately or snap frozen and stored at -80°C until analysis. Plasma interleukin 6 (IL-6) was measured by ELISA using U-PLEX Mouse IL-6 Assay® (Meso Scale Discovery, USA) and TNFα, IL1β, GM-CSF as well as INFγ were measured by ELISA using a V-PLEX custom mouse cytokine assay (#K152A0H-1, Meso Scale Discovery, USA). Ferritin was measured with a mouse Ferritin ELISA kit (Crystal Chem, Inc., USA) and hepcidin was measured in 12 µl of plasma (in duplicate) with the Hepcidin Murine-compete ELISA Kit (Intrinsic Lifesciences, USA) following the manufacturer`s instruction.

FACS analyses of hematopoietic stem cells and erythroid progenitors in bone marrow and spleen

For analyzing bone marrow hematopoiesis, a single-cell suspension of isolated bone marrow cells pooled from 2 femurs and 2 tibiae was incubated with an antibody cocktail (**Supplemental Table 2**). Lineage-positive cells were excluded using a cocktail of biotinylated antibodies (**Supplemental Table 3**) and staining with streptavidin (SA; eF450; eBioscience). Fluorescence-activated cell sorting (FACS) analysis was performed on LSRII (Becton Dickinson), and sorting was done on Aria II (Becton Dickinson). Cell numbers were counted on MACS quant. Data were analyzed with DIVA (Becton Dickinson), MACS quantify (Miltenyi), or FlowJo (Tree Star, Ashland, OR, USA). The gating strategy adopted from Pronk et al., 2007 [8] is described in **Supplemental Fig.1 A**. For analyzing erythroid progenitors in bone marrow and spleen, single-cell suspension of isolated spleen or bone marrow cells pooled from 2 femurs and 2 tibiae was incubated with an antibody cocktail (**Supplemental Table 4**) and with a Zombie Yellow™ Fixable Viability Kit (#423103, Biolegend). Cell suspension was measured by a Cytoflex S Flow Cytometer (Beckmann Coulter Life Science) and analyzed by FlowJo software (Tree Star, Ashland, OR, USA). The gating strategy adopted from Chen et. al, 2009 [9] is described in **Supplemental Fig.1 B**.

Statistics

Statistics were performed in GraphPad Prism6 (GraphPad Software, San Diego, US) Data distribution was analyzed with the Kolmogorov-Smirnov test. We used the Student‘s t-test for parametrically distributed and a Man-Whitney test for non-parametrically distributed data to compare two groups. For multiple comparisons, a one-way ANOVA with a Bonferroni`s multiple comparisons for parametrically distributed data or a Kruskal-Wallis test with a Dunn`s multiple comparisons for nonparametrically distributed data was performed. Kaplan-Meier curve was analyzed with a Log-rank (Mantel-Cox) test.

Supplemental Tables

Supplemental Table 1. Sequences of primers used for semi-quantitative real time PCR.

Gene	Primer Pair
Actb (beta-Actin)	Fwd: 5'CAACGGCTCCGGCATGTGC3'
	Rev: 5' CTCTTGCTCTGGGCCTCG 3'
Adm (Adrenomedullin)	Fwd: 5' CCGAAAGAAGTGGAATAAGTGGG 3'
	Rev: 5' GTTTGACACGAATGTGGGCT 3'
Atg3 (Autophagy related 3)	Fwd: 5'ACGGCTATGGTTGTTTGGCTATG3'
	Rev: 5'TGGTGGGAGATGAGGATGGTTT3'
Atg5 (Autophagy related 5)	Fwd: 5'CTGTCCTTCCGCAGTCGCCC3'
	Rev: 5'GTTTCCAGCATTGGCTCTATCCCGT 3'
Atg6 (Becn1, Beclin 1)	Fwd: 5'GGCTGAGGCGGAGAGATTGG3'
	Rev: 5'AGATGTGGAAGGTGGCATTGAAGA3'
Atg7 (Autophagy related 7)	Fwd: 5'CGGTGGCTTCCTACTGTTATTG3'
	Rev: 5'CCTGCTGCTTGGGTTTCTTC3'
Atg8 (Map1lc3b, Microtubule-associated protein 1 light chain 3 beta)	Fwd: 5'CAAGTTCCTGGTGCCTGACC3'
	Rev: 5'GCCGTCTTCATCTCTCTCACTCT3'
Atg10 (autophagy related 10)	Fwd: 5'CTAAAGCAACATCACAATCGGAG3'
	Rev: 5'GTACAGCTCTTGGCATTCTTCA3'
Atg12 (autophagy related 12)	Fwd: 5'AGCATTGAGGAAGTGGAAACAAGC3'
	Rev: 5'AGCAGGACAACAACAGAGTAGCA3'
Atg16 (Atg16l1, autophagy related 16 like 1)	Fwd: 5' TCC TCT CTG CCA AGT TCC TGC T 3'
	Rev: 5' TTC CAT CTC TCG GAC CAC ACT CTC 3'
Bmp2 (Bone morphogenic protein 2)	Fwd: 5' ATG TGA GGA TTA GCA GGT CTT TG 3'
	Rev: 5' GCT TCC GCT GTT TGT GTT TG 3'
Bmp6 (Bone morphogenic protein 6)	Fwd: 5' TGTGATGGAGAGTGTTCC 3'
	Rev: 5' GGCATTCAGTTTGGTTGG 3'
Creb1 (Cyclic AMP-Responsive Element-Binding Protein 1)	Fwd: 5' CAGCACGGAAGAGAGAGGTC 3'
	Rev: 5' TCTGATTTGTGGCAGTAAAGGT 3'
Creb3l1 (CAMP Responsive Element Binding Protein 3 Like 1)	Fwd: 5' CCTTCTGCTGTCCTTCGCCC 3'
	Rev: 5' AGCGTGGTTGTGGAGGGTTC 3'
Csf2 (Granulocyte-macrophage colony-stimulating factor)	Fwd: 5'CTCACCCATCACTGTCACCC 3'
	Rev: 5'GACGACTTCTACCTCTTCATTCAAC3'
Csf2 (Granulocyte colony-stimulating factor)	Fwd: 5' GCAGGCTCTATCGGGTATTT 3'
	Rev: 5' TGGAAGGCAGAAGTGAAGG 3
Dmt1 (proton-coupled divalent metal ion transporters**)**	Fwd: 5' CTTTGCTCTCATACCCAT 3'
	Rev: 5' CAATCCTCCAGCCTATTC 3'
Egln1 (Egl-9 Family Hypoxia Inducible Factor 1)	Fwd: 5' CATTGTTGGCAGAAGGTGTG 3'

	Rev: 5’ CAAAGGACTACAGGGTCTCCA 3’
Epo (Erythropoietin)	Fwd: 5’ AGACAAAGCCATCAGTGGTC 3’
	Rev: 5’ TGTGAGTGTTCGGAGTGGAG 3’
Epor (Erythropoietin receptor)	Fwd: 5’ GTCCTCATCTCGCTGTTGCT 3’
	Rev: 5’ CAGGCCAGATCTTCTGCTG 3’
Erfe (Erythroferrone)	Fwd: 5’ AGCGAGCTCTTCACCATCTC 3’
	Rev: 5’ TGTCCAAGAAGACAGAAGTGTAGTG 3’
Fpn1 (Ferroportin)	Fwd: 5’ ACC CAT CCC CAT AGT CTC TGT 3’
	Rev: 5’ CCG TCA AAT CAA AGG ACC AA 3’
Fth1 (Ferritin heavy chain 1)	Fwd: 5’ GCCAGAACTACCACCAGGAC 3’
	Rev: 5’ TTCAGAGCCACATCATCTCG 3’
Gypa (Glycophorin A)	Fwd: 5’ ATGGCAGGGATTATCGGAAC 3’
	Rev: 5’ CACCCTCAGGAGATTGGATG 3’
Hamp1 (Hepcidin-1)	Fwd: 5’ TTCCCAGTGTGGTATCTGTTG 3’
	Rev: 5’ GGGAGGGCAGGAATAAATAAT 3’
Hba (Hemoglobin alpha chain)	Fwd: 5’ TGAAGCCCTGGAAAGGATGTTTG 3’
	Rev: 5’ CCTTCTTGCCGTGACCCTTG 3’
Hbb(Hemoglobin beta chain)	Fwd: 5’ CGATGAAGTTGGTGGTGAGG 3’
	Rev: 5’ ATAGCAGAGGCAGAGGATAGG 3’
Hfe (Homeostatic iron regulator)	Fwd: 5’ TGCTACCTAACGGGGATGAG 3’
	Rev: 5’ GACGGTGACTCCACTGATGA 3’
Hjv (Hemojuvelin)	Fwd: 5’TTGCTAGATAACGACTTCCTCTTTG3’
	Rev: 5’AGCCTGGTAGACTTTCTGGT3’
Il-1b (Interleukin-1 beta)	Fwd: 5’ CCTGTGTAATGAAAGGCA 3’
	Rev: 5’ CTGCTTGTGAGGTGCTGATG 3’
Il-6 (Interleukin-6)	Fwd: 5’CTCTGGGAAATCGTGGAAAT3’
	Rev: 5’ CCAGTTTGGTAGCATCCATC 3’
Il-6r (Interleukin-6 receptor)	Fwd: 5’ TTT GGG TTG CTT CTC TGT GTC TT 3’
	Rev: 5’ AGG TCG TCT TGC TTT CCT TCT C 3’
Pdgfb (Platelet Derived Growth Factor Subunit B)	Fwd: 5’ CCAAAGGCAAGCACCGAAAG 3’
	Rev: 5’ GGGAACAACATTATCACTCCAAGG 3’
Saa1 (Serum amyloid A1)	Fwd: 5’ GGGGAACTATGATGCTGCT 3’
	Rev: 5’ ATTGGGGTCTTTGCCACT 3’
Scf (Stem cell factor)	Fwd: 5’ TGGGAAAATAGTGGATGACCTCGTGT 3’
	Rev: 5’ CGGGACCTAATGTTGAAGAGAGCACA 3’
Socs3 (Suppressor of cytokine signaling 3)	Fwd: 5’ TCACCCACAGCAAGTTTCCC 3’
	Rev: 5’ GCTCCAGTAGAATCCGCTCTC 3’
Tmprss6 (Transmembrane serine protease 6)	Fwd: 5’ CTGCTTCTTCTGGTTTATCCT 3’
	Rev: 5’ TATGTCGTTCACACTGGCTT 3’
Tnfa (Tumor necrosis factor alpha)	Fwd: 5’ ATCAAGGACTCAAATGGGCTT 3’

	Rev: 5’ GCAACCTGACCACTCTCCCT 3’
Tfrc (Transferrin receproor-1)	Fwd: 5’ GAGACTACTTCCGTGCTACT 3’
	Rev: 5’ GGAGACTCT CTTGGAGATAC3’
Tfr2 (Transferrin receproor-2)	Fwd: 5’ CTGCGGAAGGAGATTTACAG 3’
	Rev: 5’ ACTGGGACAGGAAGTAGAAC 3’
Trf (Transferrin)	Fwd: 5’ CACACACACCGAGAGGATGA 3’
	Rev: 5’ TTCTCGTGCTCTGACACTGC 3’
Zip14 (Slc39a14 solute carrier family 39 (zinc transporter), member 14)	Fwd: 5’ TCTTCTTCAACTTCCTCTCTGCCT 3’
	Rev: 5’ GCTGTCGTTCTTCTCATCCTCCT 3’

Supplemental Table 2. Antibody cocktail to analyze bone marrow hematopoiesis.

Antibody/Supplier
c-kit (A780, 2B8; eBioscience)
Sca1 (PE-Cy5 or PE-Cy7 or PE-Cy5.5, D7; eBioscience)
CD34 (FITC, RAM34; eBioscience)
CD135 (PE or PE-Cy5, A2F10; eBioscience)
CD48 (APC, HM48-1; eBioscience)
CD150 (PE-Cy7, TC15-12F12.2; BioLegend)
CD105 (PE, 12-1051-82, ThermoFisher)
CD41 (FITC, 11-0411-82; ThermoFisher)

Supplemental Table 3. Antibody cocktail to block lineage-positive cells

Antibody/Supplier
CD3 (145-2C11; eBioscience)
CD19 (eBio1D3; eBioscience)
NK1.1 (PK136; eBioscience)
Ter119 (Terr119; eBioscience)
CD11b (M1/70; eBioscience)
Gr1 (RB6-8C5; eBioscience)
B220 (RA3-6B2; eBioscience)

Supplemental Table 4. Antibody cocktail to analyze erythroid progenitors

Antibody/Supplier
FITC anti- mouse TER-119 antibody (#16205, Biolegend)
APC-Cy™7 rat anti-mouse CD45 (#561037, BD Pharmingen™)
APC/Cyanine7 anti-mouse Ly-6G/Ly-6C (Gr-1)
APC/Cyanine7 anti-mouse Ly-6G/Ly-6C (Gr-1) antibody (#108423, Biolegend)
APC rat anti-mouse CD44 Clone IM7 (RUO) (#561862, BD Pharmingen™)

Supplemental Table 5. Clinical markers in plasma of tumor free and terminal stage tumor bearing (maximal permitted tumor size) Trp53^{flox}WpCre mice.

Parameter	Tumor free	Terminal stage
Bilirubin (mg/dl)	< 0.18 ± 0.058	< 0.24 ± 0.1261
Glucose (mg/dl)	186.20 ± 28.59	163.40 ± 30.84 *
Urea (mg/dl)	36.18 ± 2.906	31.62 ± 4.155
Creatinine (mg/dl)	< 0.17 ± 0.0	<0.17 ± 0.0
Total protein (g/l)	40.43 ± 1.718	50.00 ± 7.371 **
Cholesterol (mg/dl)	106.30 ± 8.025	116.60 ± 42.14
Triglycerides (mg/dl)	191.90 ± 49.27	202.20 ± 182.7
Alkaline phosphatase (AP) (IU/l)	89.00 ± 7.321	30.50 ± 11.61 ***
Aspartate transaminase (AST) (IU/l)	496.70 ± 473.4	173.40 ± 97.57
Alanine transaminase (ALT) IU/l	39.57 ± 18.86	21.57 ± 6.705 *

Values presented as mean ± standard deviation; terminal stage is termination of experiment when maximal permitted tumor size was reached. A Mann Whitney test was performed for Bilirubin, Cholesterol and Triglycerides and all other parameters were analyzed with a student`s t test (n=7). *p<0.05; **p<0.01; ****p<0,0001.

Supplemental Figures

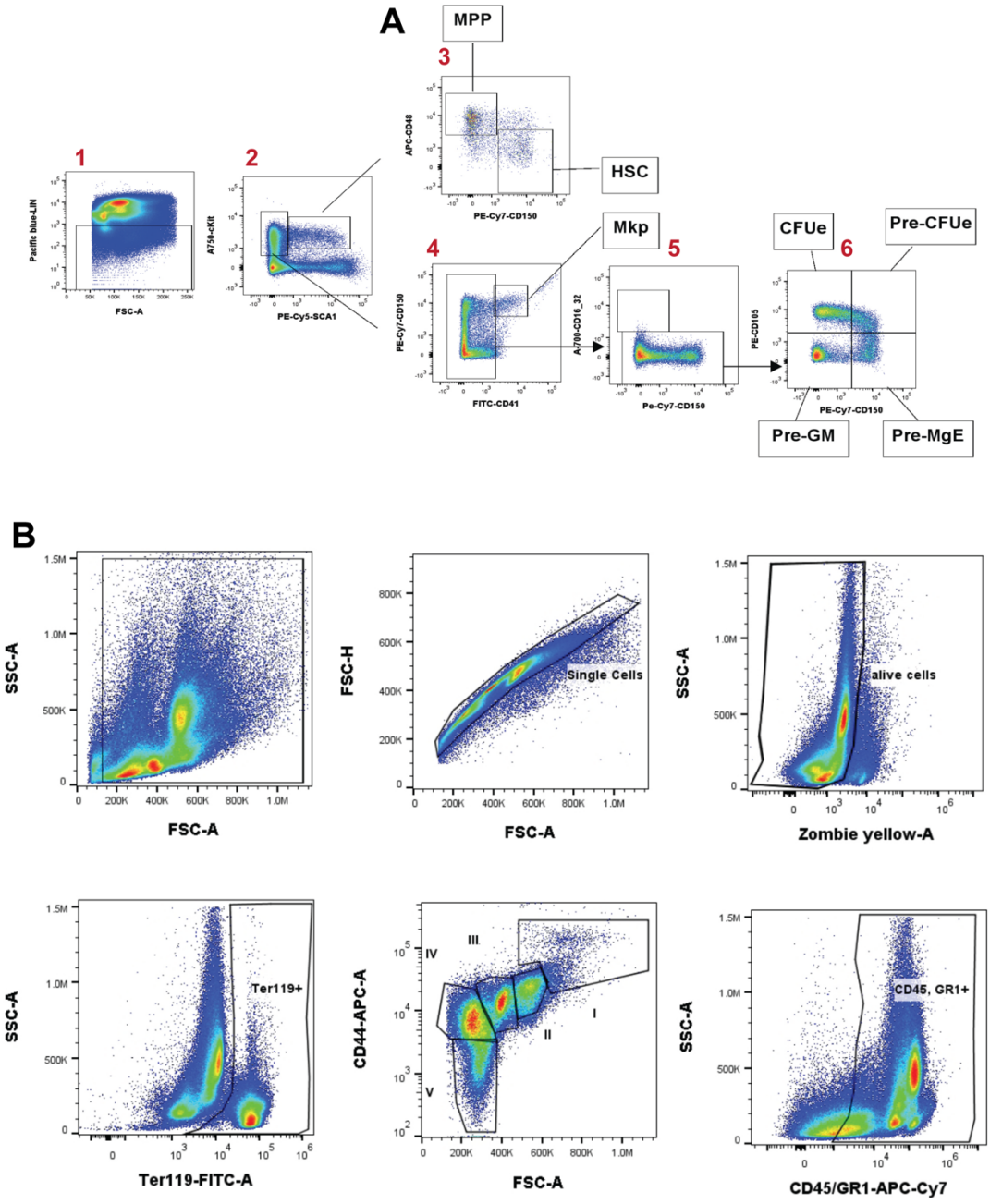

Supplemental Figure 1. Flow cytometry analysis of early and late erythroid maturation. (**A**) Shown are representative images of gated plots and the gating strategy used for flow cytometry analysis of early hematopoietic precursors in bone marrow. (1) Lineage negative (Lin^-) cells were selected for subsequent gating of (2) $C\text{-}kit^+/SCA\text{-}1^+$ cells followed by gating of (3) $CD48^-/CD150^+$ hematopoietic stem cells (HSC) as well $CD48^+/CD150^-$ multipotent progenitors (MPP). From (2) $C\text{-}kit^+/SCA\text{-}1^-$ events, (4) $CD150^+/CD41^+$ cells were considered megakaryocyte precursors (Mkp). $CD41^-$ events were selected for a (5) CD16_32/CD105 plot

and CD16_32^{-} cells were further selected for (6) a CD105/CD150 plot to identify CD105^{-}/CD150^{-} pre-granulocyte-monocyte lineage cells (Pre-GM), CD105^{-}/CD150^{+} pre-megakaryocyte-erythrocyte progenitors (pre-MgE), CD105^{+}/CD150^{+} pre-colony forming units erythrocyte (pre-CFUe) and CD105^{+}/CD150^{-} colony forming units erythrocyte (CFUe). (**B**) Shown are representative images of gated plots and the gating strategy for analyzing erythroid maturation (late erythroid progenitors) and leukocyte precursors in bone marrow and spleen by flow cytometry. Cells were gated in a forward scatter (FSC-Area, cell size) vs. side scatter (SSC-Area, cell complexity) (upper left panel) and single cells were subsequently gated in FSC-Area vs. FSC-Height plot (upper middle panel). Living cells were selected by a Zombie Yellow (dead cell marker) vs. SSC-Area plot (upper right panel) and Ter119^{+} late erythroid progenitors were gated on living cells in a Ter119 vs. SSC-Area plot (lower left panel). Different clusters were identified in FSC-Area vs. CD44 plot and based on cell size and CD44 expression (both decrease during maturation) different stages of late erythroid maturation were gated: (I) proerythroblasts, (II) basophilic erythroblasts, (III) polychromatic erythroblasts, (IV) orthochromatic erythroblasts (including reticulocytes) and (VI) mature erythrocytes (lower middle panel). Additionally, shown is the gating of CD45/GR1+ leukocyte precursors in a CD45/GR1 vs. SSC-Area plot (lower right panel).

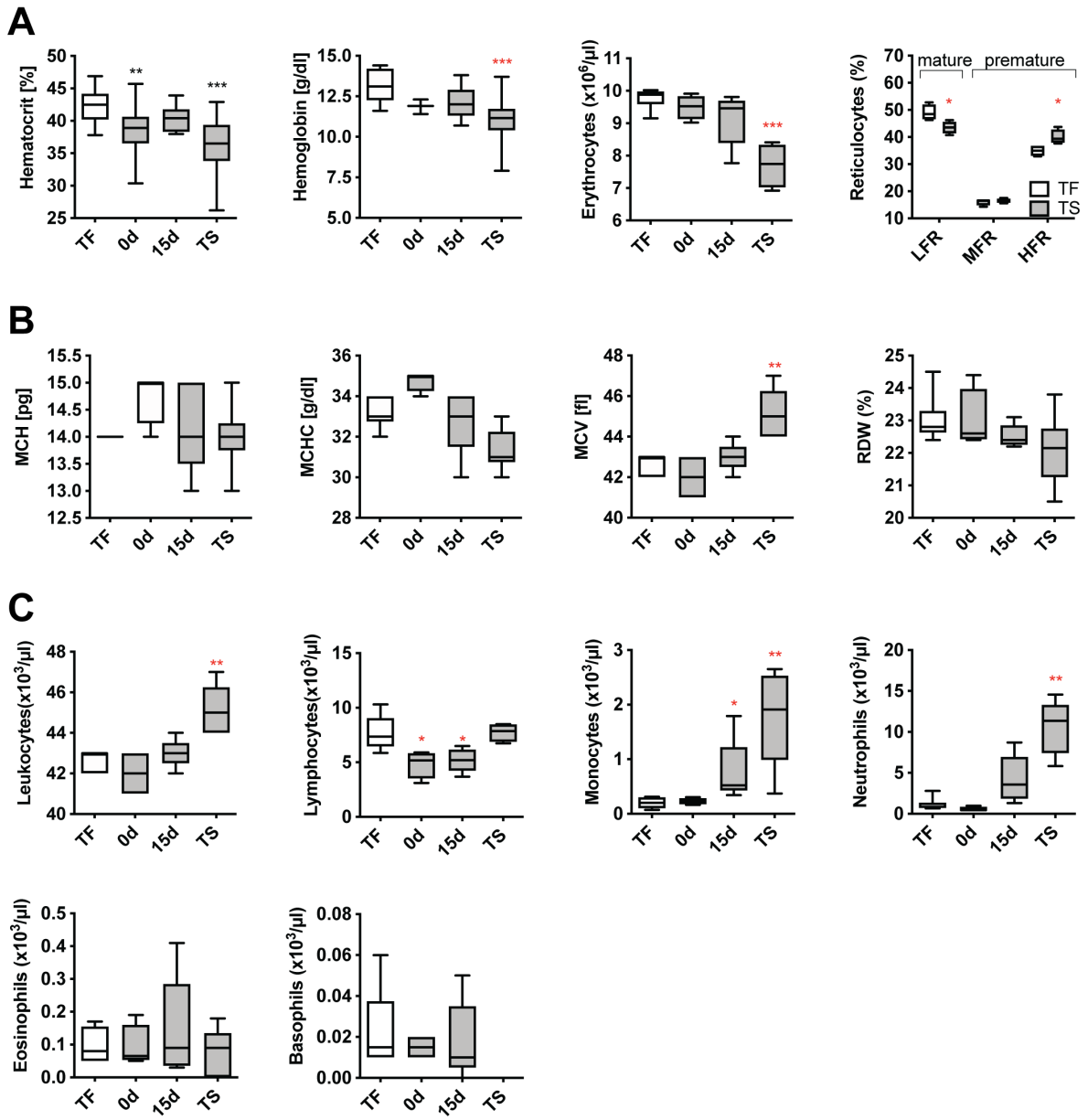

Supplemental Figure 2. Hematological analyses of anemic Trp53^{flox}WapCre mice. Blood of tumor bearing Trp53^{flox}WapCre mice (grey boxes) was isolated immediately after tumor onset (0d), 15 days after tumor onset (15d) and when the tumor reached maximal permitted size (defined as terminal stage; TS). Age-matched tumor free (TF) Trp53^{flox}WapCre mice (white boxes) served as control. Except hematocrit and hemoglobin, all parameters were analyzed by the Sysmex XT-2000iV. (**A**) Shown are hematocrit (n=11-37) and hemoglobin (n=3-39), analyzed by microcentrifugation and by ABL800, respectively. Further shown are erythrocyte count per µl blood as well as the proportion of low (LFR), middle (MFR) and high fluorescent reticulocytes (HFR) (n=4). The combined counts of HFR and MFR correspond to premature and LFR corresponds to mature reticulocytes (right panel). (**B**) Shown are mean corpuscular hemoglobin (MCH), mean corpuscular hemoglobin concentration (MCHC), mean

corpuscular volume (MCV), and red cell distribution width (RDW) (n=4-6). (**C**) Shown are the number of leukocytes per µl blood as well as the cell count per µl blood of lymphocytes, monocytes, neutrophils, eosinophils, and basophiles (n=4-6). Data are shown as box plot with min to max whiskers and data were analyzed by a one-way ANOVA with a Bonferroni`s multiple comparison (black symbols) or Kruskal-Wallis test with a Dunn`s multiple comparisons (red symbols). Reticulocytes in panel (A) were analyzed by a Mann-Whitney test (red symbols) (*p<0.05, **p<0.01, ***p<0.001).

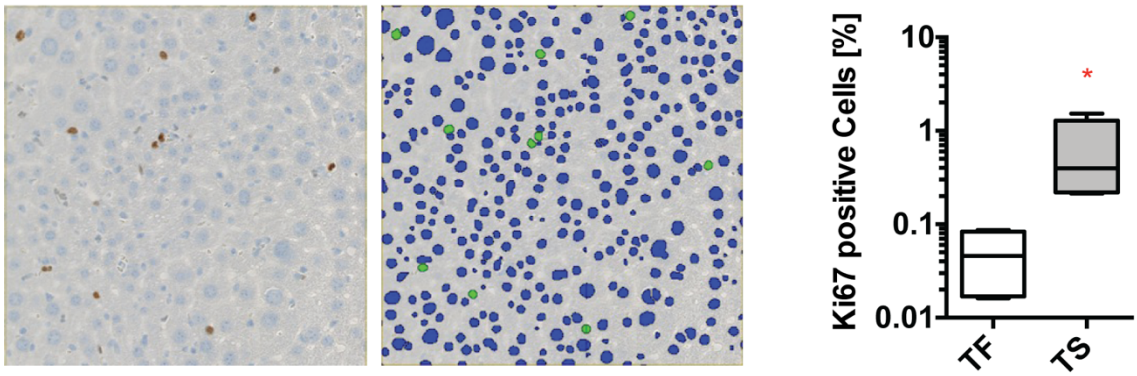

Supplemental Figure 3. Hepato- and splenomegaly in anemic Trp53^{flox}WapCre mice. Liver of tumor bearing Trp53^{flox}WapCre mice (grey boxes) was isolated, and immunohistochemically analyzed. Shown is a representative image of an immunohistochemical staining of Ki67 in the liver (left image) as well as a representative image of the morphometric quantification of Ki67 positive (green) and Ki68 negative (blue) liver cells by Visiopharm (right image). Further shown is the percentage of Ki67 positive liver cells in TF and TS mice (n=4). Data are shown as box plot with min to max whiskers. A Mann-Whitney test was performed. *p<0.05

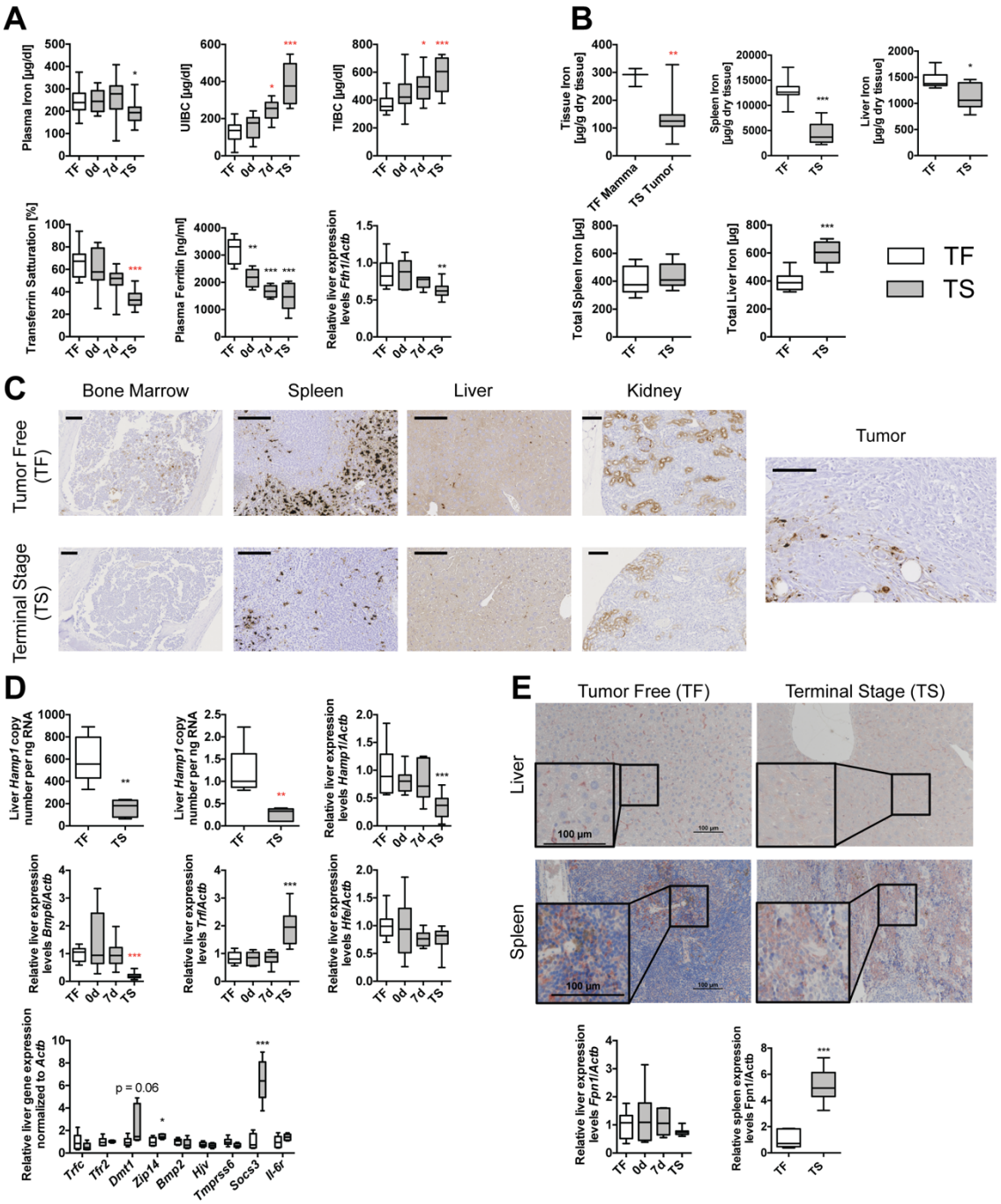

Supplemental Figure 4. Iron homeostasis in Trp53^{flox}WapCre mice. Tissues of tumor bearing Trp53^{flox}WapCre mice (grey boxes) were isolated immediately after tumor onset (0d), 7 days after tumor onset (7d) and when the tumor reached maximal permitted size (defined as terminal stage; TS). Age-matched tumor free (TF) Trp53^{flox}WapCre mice (white boxes) served as control. (**A**) Shown are plasma iron, unsaturated iron binding capacity (UIBC), total iron binding capacity (TIBC), and transferrin saturation (n=9-22) analyzed by a bathophenanthroline assay as well as plasma ferritin analyzed by ELISA (n=6) and relative liver gene expression levels of ferritin heavy chain 1 (*Fth1*) quantified by qPCR and normalized

to β-actin (*Actb*) (n=5-11). (**B**) Shown is the tissue iron concentration per dry tissue weight determined by bathophenanthroline assay in healthy mammary tissue of tumor free mice (TF Mamma) and in tumor tissue of terminal stage (TS) mice (n=3-24) as well as in spleen and liver of TF and TS mice (n=8-9). (**C**) Shown are representative images of bone marrow, spleen, liver and kidney of TS and TF mice as well as tumor tissue of terminal stage TS) $Trp53^{flox}$WapCre mice. Tissue sections were stained with DAB-enhanced Perls' to visualize iron (dark brown color). (**D**) Shown are the absolute hepcidin (*Hamp1*) mRNA copy number per ng RNA as well as *Hamp1* mRNA copy number normalized to β-actin (*Actb*) copy number determined by digital droplet PCR. Further shown are the relative liver gene expression levels of (*Hamp1*), bone morphogenetic protein 6 (*Bmp6*), transferrin (*Trf*), homeostatic iron regulator (*Hfe*), as well as transferrin receptor 1 (*Tfrc*) and 2 (*Tfr2*), divalent metal transporter 1 (*Dmt1*), solute carrier family 39 member 14/metal cation symporter ZIP14 (*Zip14*), bone morphogenetic protein 2 (*Bmp2*), hemojuvelin (*Hjv*), transmembrane serine protease 6 (*Tmprss6*), suppressor of cytokine signaling 3 (*Socs3*), and interleukin-6 receptor (*Il-6r*) quantified by qPCR and normalized to *Actb (n=5-11)*. (**E**) Shown are representative liver sections (upper images) and spleen sections (lower images) of immunohistological analyzed ferroportin (FPN1) protein expression in tumor free (left panel) and terminal stage mice (right panel) (n=3) as well as relative liver (left graph) and spleen (right graph) gene expression levels of ferroportin (*Fpn1*) quantified by qPCR and normalized to *Actb (n=6-9)*. Data are shown as box plot with min to max whiskers. Data were analyzed by a Student`s t-test (black symbols, p-values) or a Mann-Whitney test (red symbols) for single comparison or by a one-way ANOVA with a Bonferroni`s multiple comparison test (black symbols) or a Kruskal-Wallis test with a Dunn`s multiple comparison test (red symbols) (***$p<0.001$; **$p<0.01$; *$p<0.05$). Scale bar 100 µm.

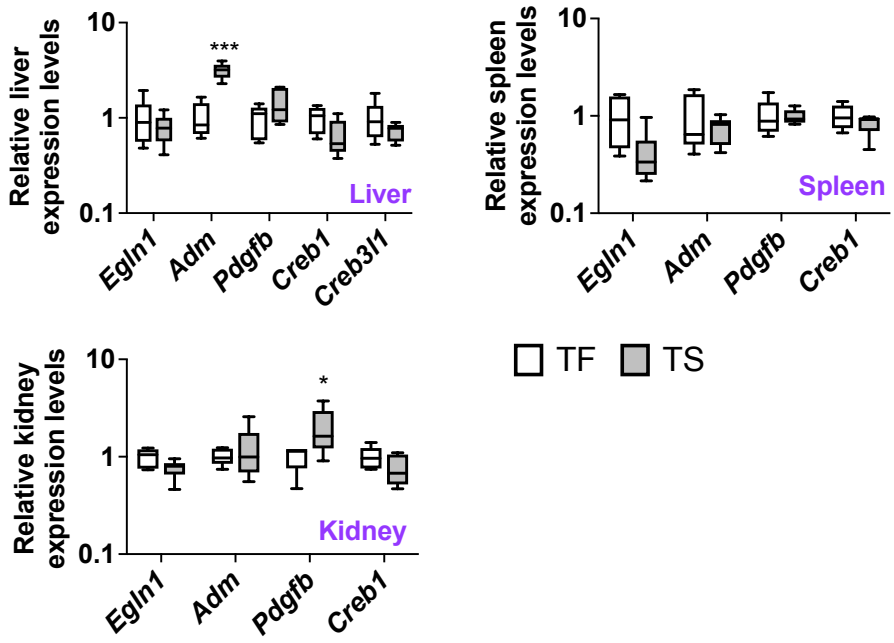

Supplemental Figure 5. Expression levels of hypoxia inducible transcription factors downstream targets and platelet derived growth factor BB in anemic Trp53^{flox}WapCre mice. Liver, spleen, and kidney of tumor bearing Trp53^{flox}WapCre mice (grey boxes) were isolated from mice when the tumor reached maximal permitted size (defined as terminal stage; TS) and from tumor free (TF, white boxes) age-matched controls. Shown are relative mRNA expression levels of hypoxia target genes Egl-9 family hypoxia inducible factor 1 (*Egln1*) and adrenomedullin (*Adm*) as well as platelet derived growth factor subunit b (*Pdgfb*) and PDGF-BB downstream target genes Camp-responsive element binding protein (*Creb1*) and Camp-responsive element binding protein 3 like 1 (*Creb3l1*) [10] in liver (upper left panel), spleen (upper right panel), and kidney (lower left panel) of tumor free (TF, white boxes) and terminal stage (TS, grey boxes) Trp53^{flox}WapCre mice. Data are shown as box plot with min to max whiskers and were analyzed by a Student`s t-test (***p<0.001; **p<0.01; *p<0.05).

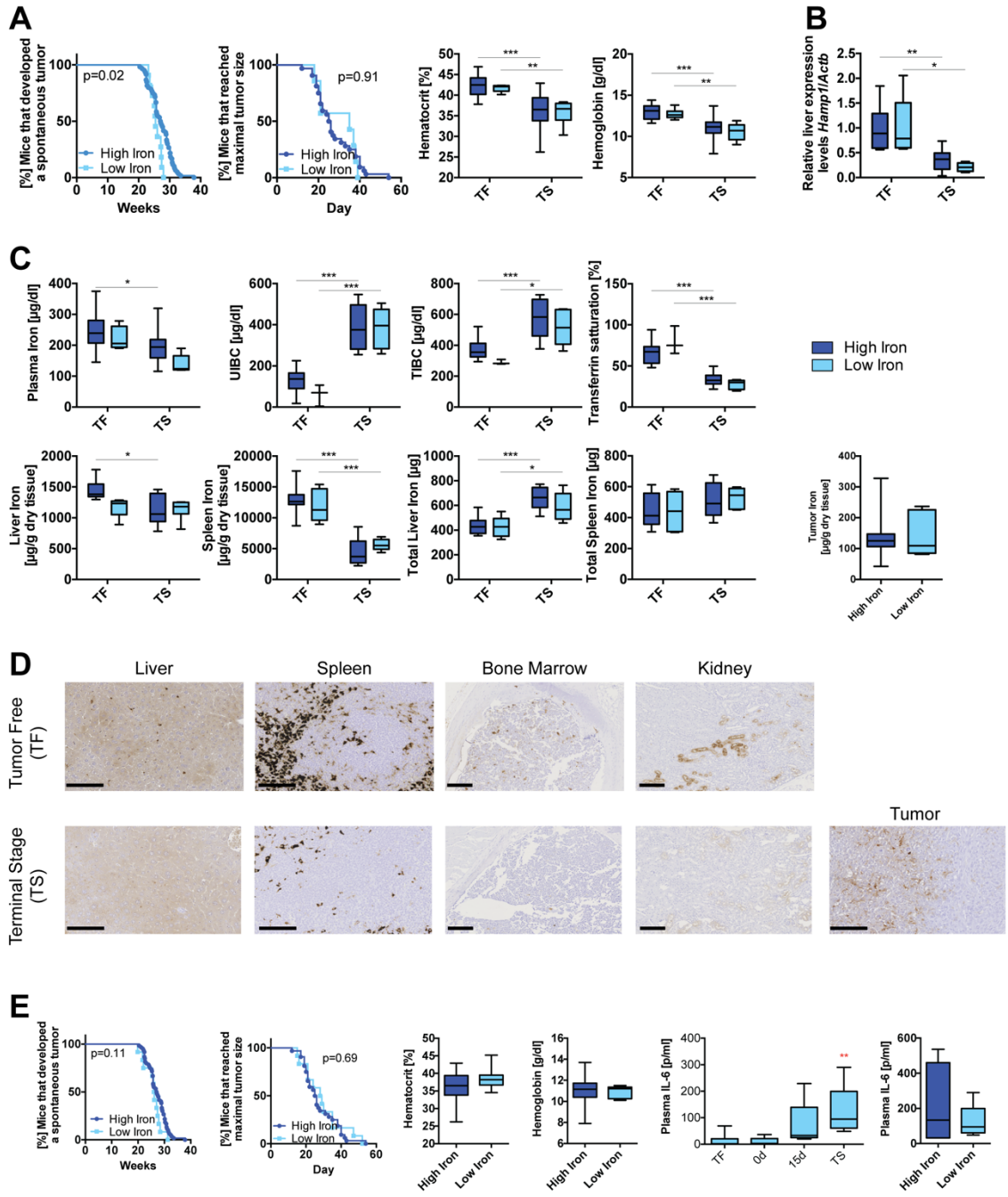

Supplemental Figure 6. Effect of low iron diet on anemia in Trp53^{flox}WapCre mice. In panel (**A-D**), Trp53^{flox}WapCre mice were kept on a standard diet with high iron content (iron 250 mg/kg). When the mice were 15 weeks of age, they either continued on the high iron diet (dark blue boxes) or they were placed on a low iron diet (50 mg/kg) (light blue boxes) until the end of the experiment. Tissues and blood of terminal stage mice (TS) were isolated when the tumor reached maximal permitted size. Age-matched tumor free Trp53^{flox}WapCre mice (TF) served as control. (**A**) Shown are modified Kaplan-Meier curves that show percentage of Trp53^{flox}WapCre mice on a low (light blue) or high (dark blue) iron diet, which developed tumors (incidence) (n=11-60) and, which reached the terminal stage (n=7-32). Data were

analyzed with a Log-rank (Mantel-Cox) test. Further shown is hematocrit and hemoglobin analyzed by microcentrifugation and by ABL800, respectively (n=6-37). (**B**) Shown is liver gene expression of Hepcidin 1 (*Hamp1*) quantified by qPCR and normalized to β-actin (*Actb*) mRNA expression (n=4-10). (**C**) Shown are plasma iron levels, unsaturated iron binding capacity (UIBC), total iron binding capacity (TIBC), and transferrin saturation quantified by a bathophenanthroline assay (n=4-22). Further shown is the tissue iron concentration quantified by a bathophenanthroline assay in liver and spleen with the corresponding total iron amount in liver and spleen (n=5-9) as well as the iron concentration quantified by bathophenanthroline in tumor tissue (n=6-24). (**D**) Shown are representative images of liver, spleen bone marrow, kidney and tumor tissue sections stained with DAB-enhanced Perl's of tumor free (upper panel) and terminal stage (lower panel) Trp53^{flox}WapCre mice kept on a low iron diet.

In (**E**), Trp53^{flox}WapCre mice were kept either on a high (dark blue) or on a low iron diet (50 mg/kg) (light blue) directly after weaning until the end of the experiment. Blood of tumor mice was isolated when the tumor reached maximal permitted size (defined as terminal stage; TS). Age-matched tumor free Trp53^{flox}WapCre mice (TF) served as control. Shown are modified Kaplan-Meier curves that show percentage of Trp53^{flox}WapCre mice on a low or high iron diet, which developed tumors (incidence) (n=12-60) and, which reached the terminal stage (n=12-32). Data were analyzed with a Log-rank (Mantel-Cox) test. Further shown are hematocrit and hemoglobin analyzed by microcentrifugation and by ABL800, respectively (n=9-38). Plasma interleukin-6 (IL-6) levels of Trp53^{flox}WapCre mice on a low iron diet were analyzed by ELISA, in TF mice, immediately (0 d) and 15 days (15 d) after tumor onset as well as in terminal stage (TS mice) (n=5-7). Additionally, we compared plasma IL-6 levels in terminal stage mice on a high (dark blue) and low (light blue) iron diet (n=4-6). Data are shown as box plot with min to max whiskers and were analyzed by a Student`s t-test or a Mann-Whitney test (no significant changes) for single comparison, by a Kruskal-Wallis test with a Dunn`s multiple comparison test (red symbols) or by a two-way ANOVA with a Bonferroni`s multiple comparison test (black symbols) (***$p<0.001$; **$p<0.01$; *$p<0.05$). Scale bar 100 µm

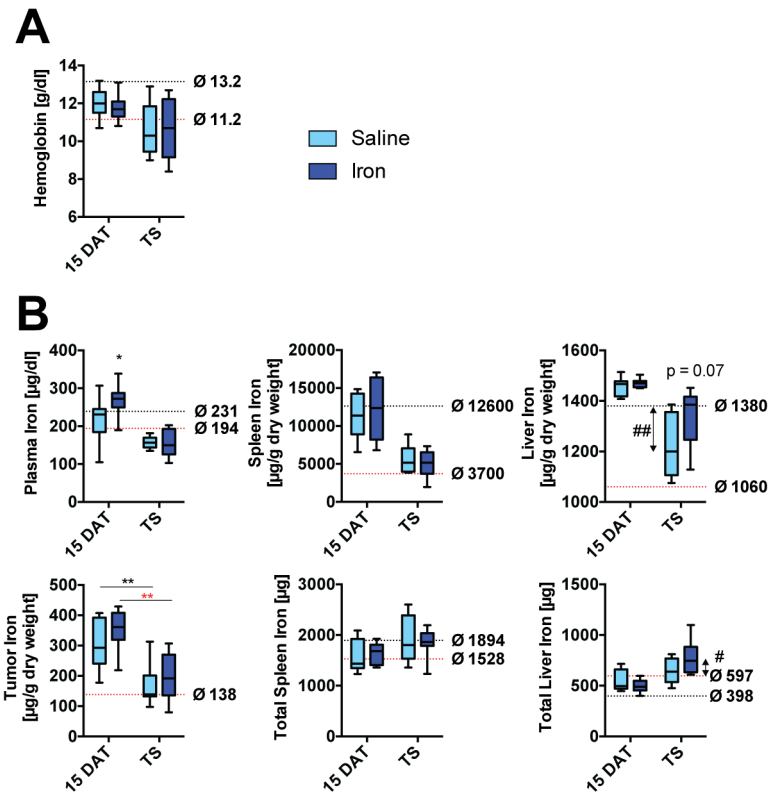

Supplemental Figure 7. Iron treatment of anemic Trp53floxWapCre breast cancer mice. Trp53^{flox}WapCre mice were intravenously injected with a single dose of iron (dark blue boxes) or saline (light blue boxes) immediately after tumor onset. In experiment 1, mice received 20 mg/kg Ferinject® and blood as well tissues were isolated 15 days after treatment (15 DAT). In experiment 2, mice received 13.28 mg/kg Ferinject® or saline and blood as well tissues were isolated when the tumor reached maximal permitted size (defined as terminal stage; TS). (**A**) Shown are hemoglobin levels in saline and iron treated mice (n=8-10). (**B**) Shown is plasma iron determined by a bathophenanthroline assay (n=5-10) (upper left panel) as well as tissue iron concentration per dry tissue weight determined by bathophenanthroline assay in spleen (upper middle panel), liver (upper right panel), and tumor (n=8-10) (lower left panel). Further shown are the corresponding total tissue iron content in spleen (lower middle panel) and liver (lower right panel) (n=8-10). Data are shown as box plot with min to max whiskers and were analyzed by a Student`s t-test (black symbols) or a Mann-Whitney test (red symbols, p-values) (***p<0.001; **p<0.01; *p<0.05). Panels with black and red dotted lines indicate the average values of untreated tumor free (black dotted line) and terminal stage (red dotted line) mice. ## and # indicates differences (p<0.01 or 0.05) between saline treated TS and untreated tumor free (black dotted line) mice and iron treated TS mice and untreated TS mice (red line), respectively.

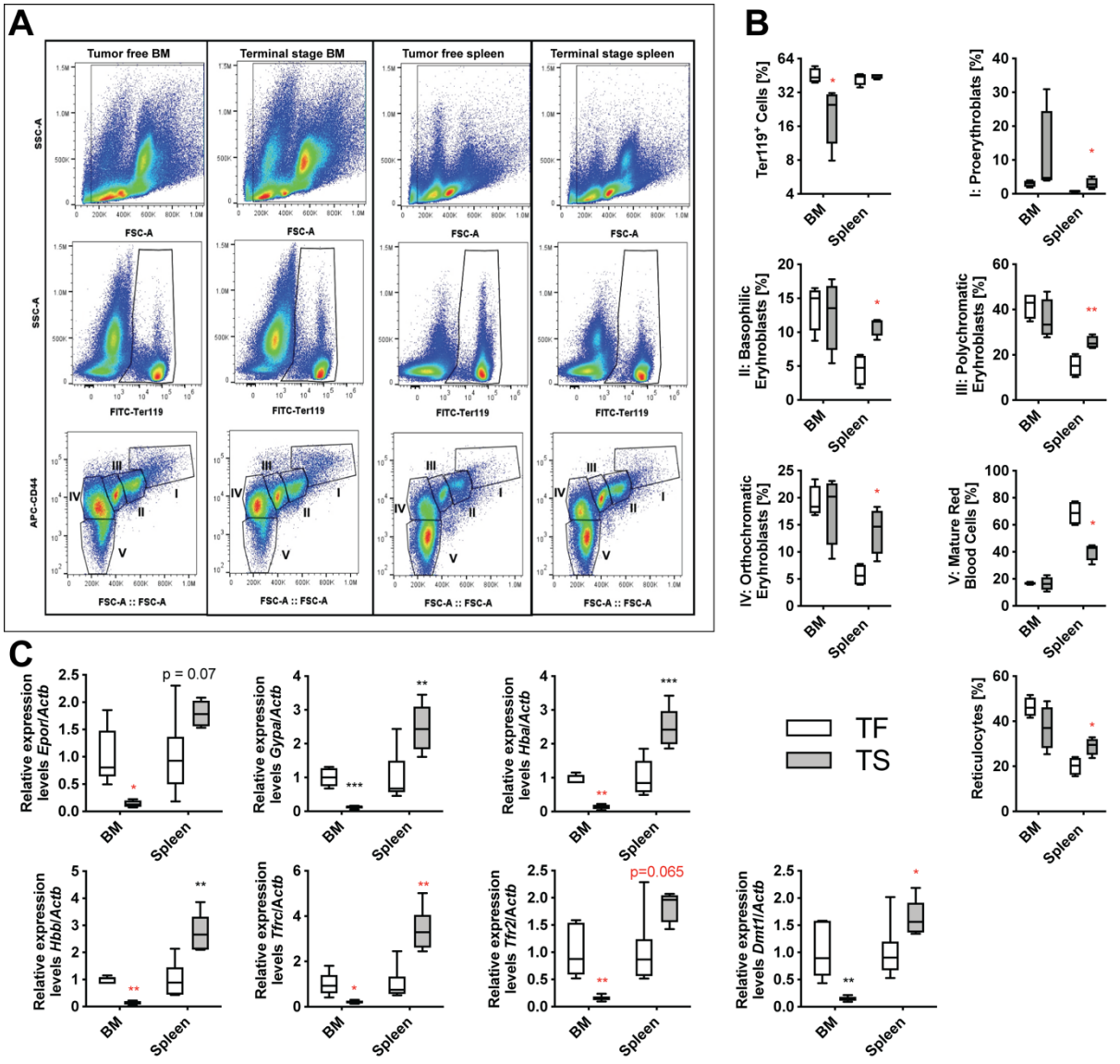

Supplemental Figure 8. Erythropoiesis in anemic Trp53^{flox}WapCre mice. Spleen and bone marrow cells of tumor bearing Trp53^{flox}WapCre mice (grey boxes) were isolated when the tumor reached maximal permitted size (defined as terminal stage; TS). Age-matched tumor free (TF) Trp53^{flox}WapCre mice (white boxes) served as control. (**A**) Shown are representative images gated plots to assess late erythroid maturation in bone marrow (BM) and spleen of tumor free and terminal stage Trp53^{flox}WapCre mice. After gating Terr119^{+} cells (middle images) clusters of differently maturated erythroid cells were identified in an FSC-Area vs. CD44 plot: (I) proerythroblasts, (II) basophilic erythroblasts, (III) polychromatic erythroblasts, (IV) orthochromatic erythroblasts (including reticulocytes) and (V) mature erythrocytes. (**B**) Shown is the proportion of Ter119^{+} in bone marrow (BM) and spleen as well as the proportion of I proerythroblasts, II basophilic erythroblasts, III polychromatic erythroblasts, IV orthochromatic erythroblasts (including reticulocytes) and V mature red blood cells in bone

marrow (BM) and spleen analyzed by flow cytometry (n=4). (**C**) Shown are relative expression levels of erythropoietin receptor (*Epor*), glycophorin A (*Gypa*), hemoglobin subunit alpha 1 (*Hba*), hemoglobin subunit beta (*Hbb*), transferrin receptor 1 (*Tfrc*), transferrin receptor *Tfr2,* and the divalent metal transporter (*Dmt1*) in bone marrow (BM) and spleen quantified by qPCR and normalized to β-actin *Actb (n=4-6)*. Data are shown as box plot with min to max whiskers and were analyzed by a Student`s t-test (black symbols, p-values) or a Mann-Whitney test (red symbols, p-values) (*p<0.05, **p<0.05).

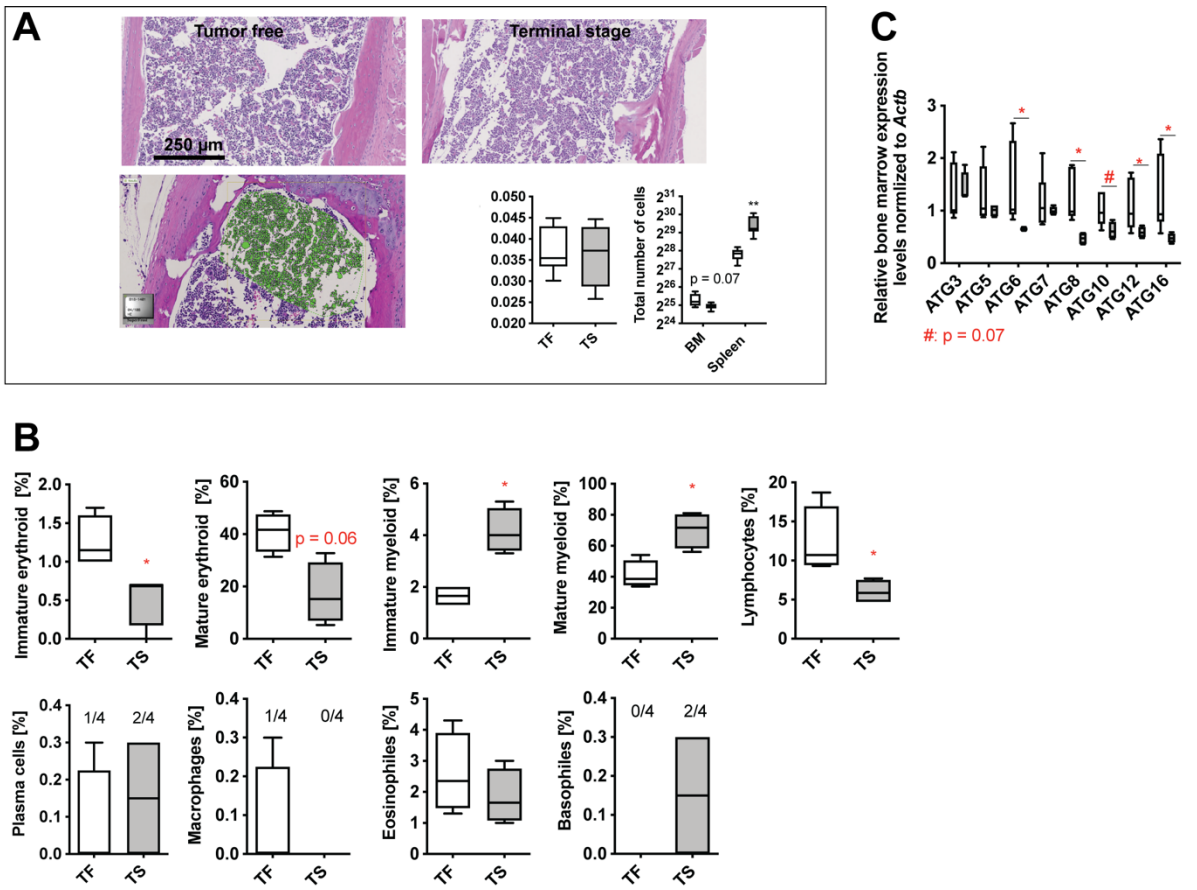

Supplemental Figure 9. Myelopoiesis in anemic Trp53^{flox}WapCre mice. Spleen and bone marrow cells of tumor bearing Trp53^{flox}WapCre mice (grey boxes) were isolated when the tumor reached maximal permitted size (defined as terminal stage; TS). Age-matched tumor free (TF) Trp53^{flox}WapCre mice (white boxes) served as control. (**A**) Shown are representative bone marrow sections of tumor free (upper left image) and terminal stage (upper right image) stained with hematoxylin-eosin. The lower image shows a representative image of the morphometric quantification of bone marrow cells (green). Further shown are the cellularity in bone marrow tissue sections analyzed by Visiopharm (n=6) as well as cellularity in bone

marrow (BM) and spleen analyzed by flow cytometry (n=5-8). (**B**) Shown is the proportion of immature and mature erythroid precursors, immature and mature myeloid precursors, lymphocytes, plasma cells, macrophages, eosinophils, and basophils in Giemsa-stained bone marrow smears (n=4). (**C**) Shown are relative expression levels of autophagy genes in bone marrow of tumor free (white boxes) and terminal stage $Trp53^{flox}$WapCre mice (grey boxes) analyzed by qPCR and normalized to β-actin (*Actb*) (n=4-6). Data are shown as box plot with min to max whiskers and were analyzed by a Student`s t-test (black symbols, p-values) or a Mann-Whitney test (red symbols, p-values) (*$p<0.05$, **$p<0.05$).Scale bar 250 µm

References

1. Jonkers J, Meuwissen R, van der Gulden H, et al. Synergistic tumor suppressor activity of BRCA2 and p53 in a conditional mouse model for breast cancer. Nat Genet. 2001;29(4):418-425.

2. Faustino-Rocha A, Oliveira PA, Pinho-Oliveira J, et al. Estimation of rat mammary tumor volume using caliper and ultrasonography measurements. Lab Anim (NY). 2013;42(6):217-224.

3. Ganzoni AM. [Intravenous iron-dextran: therapeutic and experimental possibilities]. Schweiz Med Wochenschr. 1970;100(7):301-303. Eisen-Dextran intravenos: therapeutische und experimentelle Moglichkeiten.

4. Torrance JD, Bothwell TH. A simple technique for measuring storage iron concentrations in formalinised liver samples. S Afr J Med Sci. 1968;33(1):9-11.

5. Reagan WJ, Irizarry-Rovira A, Poitout-Belissent F, et al. Best practices for evaluation of bone marrow in nonclinical toxicity studies. Vet Clin Pathol. 2011;40(2):119-134.

6. Thornton B, Basu C. Real-time PCR (qPCR) primer design using free online software. Biochem Mol Biol Educ. 2011;39(2):145-154.

7. Livak KJ, Schmittgen TD. Analysis of relative gene expression data using real-time quantitative PCR and the 2(-Delta Delta C(T)) Method. Methods. 2001;25(4):402-408.

8. Pronk CJ, Rossi DJ, Mansson R, et al. Elucidation of the phenotypic, functional, and molecular topography of a myeloerythroid progenitor cell hierarchy. Cell Stem Cell. 2007;1(4):428-442.

9. Chen K, Liu J, Heck S, et al. Resolving the distinct stages in erythroid differentiation based on dynamic changes in membrane protein expression during erythropoiesis. Proc Natl Acad Sci U S A. 2009;106(41):17413-17418.

10. Sonnweber T, Nachbaur D, Schroll A, et al. Hypoxia induced downregulation of hepcidin is mediated by platelet derived growth factor BB. Gut. 2014;63(12):1951-1959.